New Mode-Group-Permutation Strategies for MDL Reduction in Long-Haul MDM Systems

Huihui Wang[1], Xutao Wang[1], Yichen He[1], Zhiqun Yang[1*], Yaping Liu[1*], Qiang Guo[2], Rui Zhou[2], Xinhua Xiao[2], Zhanhua Huang[1], and Lin Zhang[1,3*]

[1]*Key Laboratory of Opto-electronic Information Technology of Ministry of Education and Tianjin Key Laboratory of Integrated Opto-electronics Technologies and Devices, School of Precision Instruments and Opto-electronics Engineering, Tianjin University, Tianjin, 300072, China*
[2]*B&P Laboratory, Huawei Technologies Co., Ltd., Shenzhen 518129, China*
[3]*Peng Cheng Laboratory, Shenzhen 518038, China*
**Corresponding authors: yangzhiqun@tju.edu.cn, liuyp@tju.edu.cn, lin_zhang@tju.edu.cn*

Abstract: We compare 9 types of mode-permutation strategies (MPSs) aiming at MDL reduction in MDM systems, based on in-house low-DMD 6-mode optical fibers and MPLCs. Two new CMGP strategies are proposed, showing reach extension by 3~3.5 times.

1. Introduction

Space-division multiplexing (SDM) using fibers with multiple cores [1] and/or multiple modes has been introduced to increase optical communication system capacity [2]. As one of the significant linear impairments of SDM components or systems, mode-dependent loss (MDL) directly limits system capacity as it leads to signal-to-noise ratio degradation, which is hard to be recovered through multiple-input multiple-output processing [3]. As shown in Fig. 1(a), in conventional mode-division multiplexing (MDM) systems, the overall MDL grows almost linearly with fiber length. It leads to significantly limited transmission distances.

To reduce MDL and differential mode delay (DMD) in long-haul transmission, it is necessary to properly balance performances of spatial channels. Cyclic mode permutation (CMP) was proposed to suppress DMD-induced impact and mitigate MDL effect, in which spatial mode signals are cyclically shifted after each span [4, 5]. A 6-mode MDM transmission system over 3250 km has been reported [5]. However, mode-to-mode averaged performance in this configuration might not be discounted because of the degenerate modes in a mode group [6]. Later, a scheme that considers mode-group granularity was proposed [6], termed cyclic mode-group permutation (CMGP), which enables 3-mode MDM transmission over >6000 km. A recently proposed mirror-flipped mode permutation (MFMP) employs the symmetric group delay characteristics of new 6-mode FMFs [7] and enables mode exchanging more frequently to alleviate DMD and MDL, demonstrating 1028-km MDM transmission [7]. Although these channel permutation schemes exhibit greatly leveraged transmission performance, there are still many permutation strategies remaining unexplored, and a careful comparison especially with real FMFs and mode permutation devices is urgently needed to provide design guidelines for long-haul MDM transmission systems.

Here, we compare 9 types of mode-permutation strategies (MPSs), i.e., the 3 existing strategies mentioned above, 3 CMP's variants (named CMP.X) and 3 CMGP's variants (named CMGP.X), aiming at a greatly reduced MDL. The transmission matrices and MDLs of both 6-mode optical fibers and the mode permutation device (MPD) are measured using a swept-wavelength interferometer (SWI) [8]. Based on the measurements, further analyses on long-haul transmission are carried out. In this way, it is revealed that, at a certain MDL level, two newly explored MPSs, i.e., CMGP.B and CMGP.C, outperform with a reach extension by 3~3.5 times, compared with that without permutation.

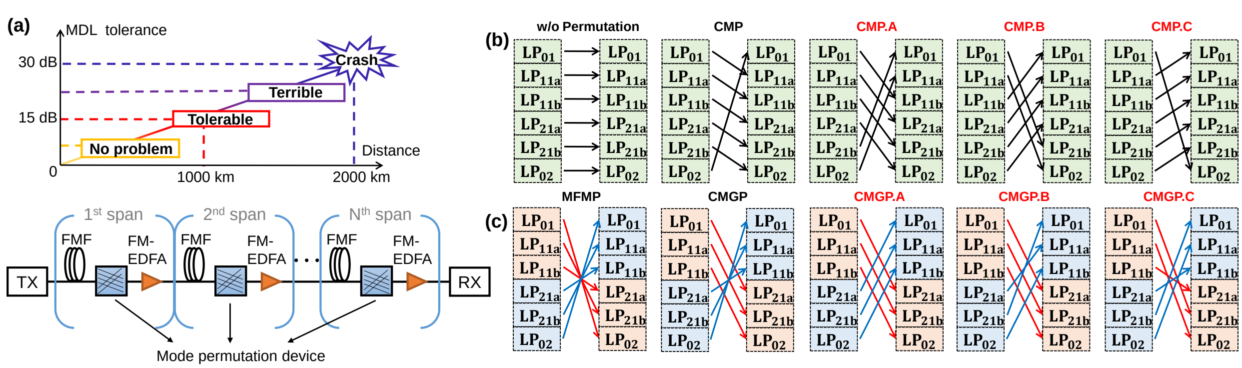

Fig. 1. (a) MDL accumulates linearly with transmission distance, and in an MDM transmission link, mode permutation devices are inserted at the ends of spans. (b) CMP and new CMP variants (named CMP.X), (c) MFMP, CMGP, and new CMGP variants (named CMGP.X), colored according to mode groups.

2. Newly explored CMP.X and CMGP.X schemes

Mode permutation is proposed to balance the performance of the individual space channels [4-7], which means that each mode signal would be transformed to another mode signal before entering the next span via a mode-selective multiplexer/demultiplexer pair. Therefore, after transmission over several spans, the information symbols are expected to periodically experience each spatial channel. Different MPSs could mitigate the effects of MDL in long-haul transmission with different performances.

After careful selection, we decide to consider the comparison of nine MPSs for a 6-mode transmission as shown in Fig. 1(b)&(c). The latter three ones on the first line are variants of CMP, named CMP.A, CMP.B, CMP.C, respectively, where mode signals are cyclically exchanged, taking number of the modes as the cycle. Similarly, as shown in Fig. 1(c), CMGP.A, CMGP.B, and CMGP.C are the variants of CMGP. Six spatial modes are categorized into two mode groups, namely, a lower-order mode group with $LP_{01}/LP_{11a}/LP_{11b}$ modes, and a higher-order mode group with $LP_{21a}/LP_{21b}/LP_{02}$ modes. Different from the existing CMGP, the CMGP.X exchanges one of the degenerate modes with one non-degenerate mode in another mode groups. Take CMGP.B as an example, signals propagated as LP_{01} mode at the p-*th* span are converted and transmitted as LP_{21a} mode at the (p+1)-*th* span.

3. Characterization of 6-mode fiber and mode permutation device

The experimental measurement setup is shown in Fig. 2(a). SWI is used to characterize the transmission matrices of the MPD. Multi-plane light conversions (MPLCs) are used to construct MPD for 6-mode exchanging as shown in the right side of Fig. 2(b).

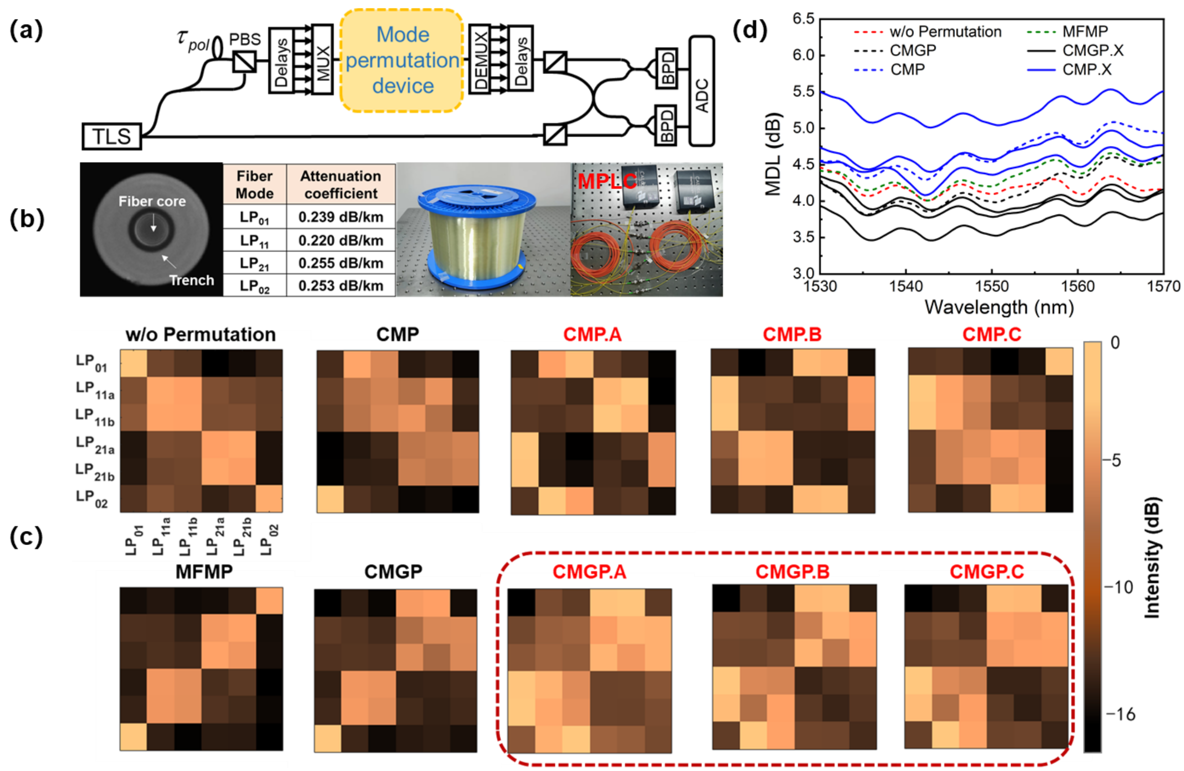

Fig. 2. (a) Experimental setup of SWI to characterize the matrices of a MPD, (b) the cross section of the 6-mode fiber, measured losses of the fiber modes, photos of the in-house fiber and MPLCs, (c) the 6×6 transfer matrices of MPDs with different MPSs, (d) measured MDL of the MPDs vs. wavelength, with different MPSs.

The 6×6 power transfer matrices was calculated from the 12×12 complex transfer matrices measured by SWI at different wavelengths for dual-polarization six modes. Figure 2(c) shows the transfer matrices of the MPD with different MPSs at 1550 nm. The column and row of each transfer matrix represent the launched modes and received modes, respectively. The transfer matrix without permutation is nearly diagonal, which indicates good mode selectivity from the SMUXs. With the addition of MPSs, LP_{01}, $LP_{11a/b}$, $LP_{21a/b}$ and LP_{02} modes are strongly mixed at 1550 nm. MDL is defined as the ratio of the maximum and minimum singular values of the complex transfer matrix. We present the measured MDL versus wavelengths of the MPD with different MPSs in Fig. 2(e). As we can see, the black curves are lower than the blue curves, indicating better MDL mitigation performance for CMGP.X.

Corresponding these curves to the power transfer matrices in Fig. 2(c), it can be found that the power distribution of CMGP.X matrices is uniform within mode groups and distributed on the off-diagonal elements. This implies that the lower-order mode group and higher-order mode group are strongly coupled, and the losses of the non-degenerate modes and degenerate modes are also balanced. Since the MDL curves fluctuate slightly over the C-band, we took the complex transfer matrices of the MPD at 1550 nm for the further evaluation of their performance in long-haul transmission systems.

4. MPS evaluation for long-haul MDM transmission

The practical transfer matrices of the MPD and the six-mode fiber measured by SWI are combined together for the evaluation of long-haul transmission performance with multi spans. The cross-section image, physical photograph, and attenuation coefficients of the fiber are shown in Fig. 2(b). We set the span lengths to be 60 km, 70 km and 80 km to exclude the influence of that. The results are shown in Fig. 3.

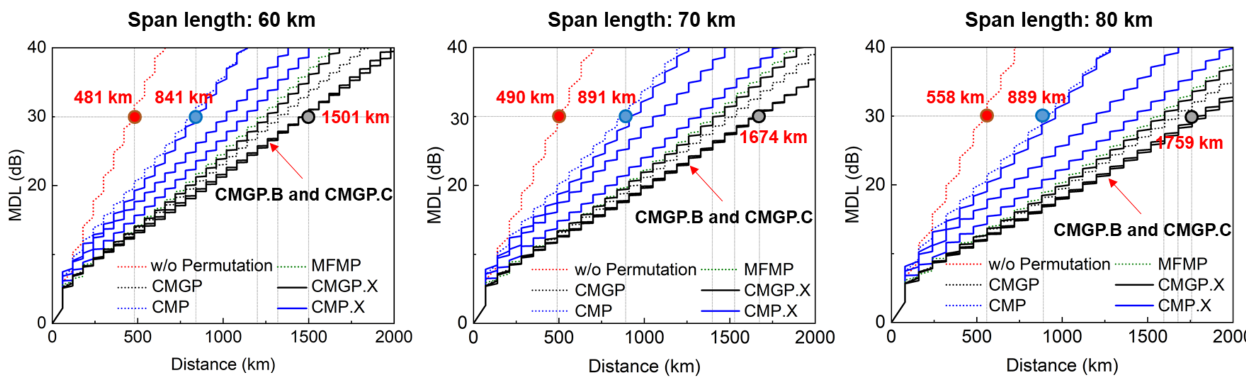

Fig. 3. Nine types of MPSs show dramatically different MDL accumulations in long-haul MDM transmission at three span lengths: 60 km, 70 km and 80 km. In particular, CMGP.B and CMGP.C presented here outperform.

MDL increases almost linearly with transmission distance without mode permutation. The stepped curve is due to the abrupt change in MDL caused by the MPDs at the beginning of each span. The growth rate varies for different MPSs. We can see that 30 dB is the limit of the current algorithm ability based on the existing simulations [9] and 20 dB is the limit of solvability according to the available experiments [10]. Thus, we set the MDL threshold to be 30 dB, and the longest transmission reach is recorded for each MPS, i.e., the intersection points in Fig. 3. The results show that the CMGP.B and CMGP.C perform better, whose transmission reach increases 3~3.5 times compared to the case without MPS. Besides, compared to CMP, the transmission distance of CMGP.B and CMGP.C improves 1.7~2 times. It should be noted that CMP.X series do not perform well. The results are consistent with the MDL measurement results of discrete MPD, indicating that it is necessary to characterize the MPD before making up a link. In addition, different span lengths have a slight effect on the performance of MPSs, and the reach of MFMP and CMGP gradually approaches that of CMGP.X as the span length increases.

5. Conclusion

We demonstrate six new MPSs based on the existing mode permutation strategies and evaluate their mitigation effect on MDL in long-haul transmission. The results show that the MDL of MPD is smaller than other MPSs when using CMGP.B and CMGP.C. Furthermore, CMGP.X series can improve the transmission reach by 3~3.5 times compared to that without MPS, and by 1.7~2 times compared to the CMP. This allows the conclusion that the evaluation and selection of different MPSs are necessary for long-haul MDM transmission links.

6. Acknowledgement

The work was supported by National Key R&D Program of China under grant 2019YFB2203902 , National Natural Science Foundation of China (NSFC) under grant 62105241, and Postgraduate Research Program of Tianjin under grant 2021YJSB129.

7. References

[1] A. V. Turukhin *et al.*, *J. Lightw. Technol.*, 35(4), 1028-1032 (2017).
[2] C. Carboni *et al.*, *Front. Optoelectron.*, 9(2), 270-276 (2016).
[3] Y. J. Chen *et al.*, in 2011 *ECOC*, Tu.6.A.1.
[4] K. Shibahara *et al.*, in 2018 *OFC*, pp. Th4C.6.
[5] K. Shibahara *et al.*, *J. Lightw. Technol.*, 37(1), 138-147 (2019).
[6] K. Shibahara *et al.*, in 2020 *OFC.*, pp. Th3H. 3.
[7] Y. Wang *et al.*, in 2022 *OFC.*, pp. M4B.5.
[8] N. K. Fontaine *et al.*, in 2013 *OFC.*, pp. OW1K.2.
[9] A. Lobato *et al.*, *Opt. Express*, 20(28), 29776-29783(2012).
[10] H. Huang *et al.*, *J. Lightw. Technol.*, 40(13), 4136-4149 (2022).